# Excision without excision

David Brown,[1] Olivier Sarbach,[2] Erik Schnetter,[3,4] Manuel Tiglio,[4,3] Peter Diener,[4,3] Ian Hawke,[5] and Denis Pollney[6]

[1] *Department of Physics, North Carolina State University, Raleigh, NC 27695, USA*
[2] *Instituto de Física y Matemáticas, Universidad Michoacana de San Nicolás de Hidalgo, Morelia, Michoacán, México*
[3] *Center for Computation & Technology, Louisiana State University, Baton Rouge, LA, USA*
[4] *Department of Physics and Astronomy, Louisiana State University, Baton Rouge, LA, USA*
[5] *School of Mathematics, University of Southampton, Southampton, UK*
[6] *Albert-Einstein-Institut, Max-Planck-Institut für Gravitationsphysik, Golm, Germany*

(Dated: July 19, 2007)

*to turducken (turduckens, turduckening, turduckened, turduckened)* [math.]: To stuff a black hole.



We analyze and apply an alternative to black hole excision based on smoothing the interior of black holes with arbitrary – possibly constraint violating – initial data, and solving the vacuum Einstein evolution equations everywhere. By deriving the constraint propagation system for our hyperbolic formulation of the BSSN evolution system we rigorously prove that the constraints propagate causally and so any constraint violations introduced inside the black holes cannot affect the exterior spacetime. (This does not follow from the causal structure of the spacetime as is often assumed.) We present numerical evolutions of Cook-Pfeiffer binary black hole initial configurations showing that these techniques appear to work robustly for generic data. We also present numerical evidence from spherically symmetric evolutions that for the gauge conditions used the same stationary end-state is approached irrespective of the choice of initial data and smoothing procedure.

PACS numbers: 04.20.-q,04.25.Dm,04.30.Db

## I. INTRODUCTION

Currently, there are essentially two different ways of dealing with singularities in the numerical evolution of orbiting black holes. One technique is black hole excision [1, 2], where the interior of each black hole is removed from the computational domain by an inner boundary. The other is the so called "moving punctures" technique [3, 4], where the initial asymptotically flat regions inside each black hole are represented by "puncture points". Long, multi-orbit binary black hole simulations have been achieved over the last few years using both excision [5, 6] and moving punctures (see [7] and references therein).

The puncture technique does not make use of the black hole excision idea, at least not in the classical sense of placing an inner boundary inside each black hole. Instead, the fields that initially describe the puncture points are allowed to evolve freely in the (topologically trivial) computational domain and the subtleties of black hole excision are replaced by the subtleties involved in approximating the singularities in the equations at the puncture points. The particular appeal of the "moving punctures" technique compared to black hole excision is that it appears to be simpler to achieve a stable discretization near the puncture points than at an excision boundary; however, there appears to be an implicit limitation of the method in that it is in principle tied to the use of puncture data. Recently, light has been shed on the geometric picture behind moving punctures [8, 9, 10].

In this paper we discuss a technique for evolving black holes which shares the simplicity of moving punctures but is not restricted to puncture-type initial data and does not need any regularization of the equations near special points. The method also relies on the intuitive idea behind black hole excision that "no physical information can escape from the interior of a black hole", but proceeds in a different way. In particular, it does not require placing an inner boundary per black hole in order to remove the interiors. The computational domain in this technique is trivial (from a topological point of view) and the discretization therefore remains simple.

The basic idea is the following: if no physical information can leave the interior of the black hole, why not just change the interior to one's advantage? The spirit of this idea is not new, and has been advocated for a long time in several forms, most notably by Bona and collaborators [11, 12, 13] and by Misner [14]. In particular, in [12], a "free black evolution" approach was advocated, where the interior of each black hole is smoothed with arbitrary data and the vacuum Einstein evolution equations are solved everywhere. In general the smoothing process generates constraint violations. Thus, a key ingredient of this approach is to guarantee that the form of the equations does not allow for constraint violations to propagate to the outside. This is highly non-trivial. In fact, it is well known that depending on the form of the Einstein equations used, gauge and constraint modes can propagate with arbitrary (including superluminal) speeds and, in particular, constraint violations *can* leak from the interior of black holes to the outside. Though we use a different formulation of the equations (a version of BSSN as opposed to the Z4 system [12]), this "free black hole evolution" approach is exactly the one that we analyze and apply in this paper. Even though in several aspects

this is different from the "stuffed black hole proposal" [11], we will refer to our particular implementation as *the relativistic turducken* [15].

## II. NO CONSTRAINT LEAKING IN THE TURDUCKENING: AN ANALYTICAL PROOF

The exact version of the BSSN system we use is given by Eqs. (3)–(7), (21)–(23) in [16] where we set the parameter $m$ to one and the source terms $S$, $\hat{S}_{ij}$ and $S^i$ to zero. Furthermore, the lapse $\alpha$ and the shift $\beta^i$ are evolved according to the $1+\log$ slicing condition $\hat{\partial}_0\alpha = -2\alpha K$ and the "hyperbolic Gamma driver" [17] like conditions $\hat{\partial}_0\beta^i = 3B^i/4$, $\hat{\partial}_0 B^i = \hat{\partial}_0\tilde{\Gamma}^i - B^i/2$ , respectively, where $\hat{\partial}_0 = \partial_t - \beta^j\partial_j$. The term $\hat{\partial}_0\tilde{\Gamma}^i$ in the last equation is set equal to the right-hand side of the evolution equations for the $\tilde{\Gamma}^i$ symbols. As noted in [16] the use of $\hat{\partial}_0$ (as opposed to $\partial_t$) in the above equations simplifies the analysis of the hyperbolic structure of the equations. Later, it was also found to be important in practice for long-term binary evolutions [18]. In addition, using $\hat{\partial}_0$ for the lapse implies that the slicing obtained is independent of the choice of shift vector [8].

The well-posedness of the resulting Cauchy problem was analyzed in [16]. A sufficient condition for well-posedness is strong hyperbolicity of the evolution equations. (See [19, 20] for definitions that apply to second order systems.) In our case, the equations are strongly hyperbolic if and only if the lapse $\alpha$ and the conformal factor $\phi$ are smooth functions satisfying $\alpha > 0$, $|\phi| < \infty$ and $h := 2\alpha - e^{4\phi} \neq 0$. The last condition is typically violated, at least on some two-surface. This is so because in general, $\alpha \to 1$ and $\phi \to 0$ and therefore $h \to 1$ as one approaches the main asymptotically flat end, while near black holes $\alpha$ is small and $\phi$ is large and positive (for the coordinate conditions used here typically $\alpha \approx 0.3$ at the horizon, and $\alpha \to 0$ and $\phi \to \infty$ at any punctures) so that $h < 0$ near a horizon. Therefore, the function $h$ must be zero somewhere in between. On the other hand, if the regions where $h = 0$ are, for example, sets of zero-measure in the computational domain there is hope that the violation of the condition $h \neq 0$ still allows for a well posed Cauchy problem. The numerical simulations in Sect. IV below show no apparent sign of numerical instability.

The characteristic speeds (with respect to normal observers) for our evolution equations are the following [16]: $0, \pm 1, \pm\mu_1, \pm\mu_2, \pm\mu_3$, where $\mu_1 = \sqrt{2/\alpha}$, $\mu_2 = \sqrt{3}\, e^{2\phi}/2\alpha$, $\mu_3 = e^{2\phi}/\alpha$. It is possible to give a precise meaning to the different characteristic fields and speeds in the high-frequency limit [21, 22]. In that limit, fields propagating with speeds $\mu_1$, $\mu_2$ and $\mu_3$ correspond to gauge modes, while the fields corresponding to gravitational radiation and constraint-violating modes have speeds $\pm 1$ and 0, $\pm 1$ respectively. As we will see below, the constraint propagation system possesses the characteristic speeds 0 and $\pm 1$.

The BSSN system is subject to the Hamiltonian and momentum constraints $H = 0$ and $M_i = 0$ plus three extra constraints associated with the introduction of the $\tilde{\Gamma}^i$ symbol as independent variables, namely $C^i_\Gamma := \tilde{\Gamma}^i + \partial_j\tilde{\gamma}^{ij} = 0$, where $\tilde{\gamma}^{ij}$ refers to the inverse of the conformal metric. In order to obtain a solution to Einstein's vacuum field equations, these constraints have to be satisfied. We now show that it is sufficient to solve them on an initial Cauchy surface in the region exterior to the black holes. The constraint propagation system then guarantees[1] that these constraints hold at every time future to the initial surface and at every point outside the black hole regions, *independent of any constraint violation in the interior of the black holes*. We show this by deriving the constraint propagation system and casting it into first order symmetric hyperbolic form. Then the causal propagation of the constraints can be shown via a standard energy inequality provided all the characteristic speeds (as measured by normal observers) of the system are smaller than or equal to one in magnitude.

Using the Bianchi identities, imposing the evolution equations and introducing the additional constraint variables $Z_{ij} = (\partial_i C^k_\Gamma)\tilde{\gamma}_{kj}$, the constraint propagation system can be rewritten as a first order system of the form

$$\hat{\partial}_0 C = \alpha\left[\mathbf{A}(u)^i\partial_i C + \mathbf{B}(u)C\right], \tag{1}$$

where $C$ are the constraint variables, $u = (\alpha, \phi, \tilde{\gamma}_{ij}, K, \tilde{A}_{ij}, \tilde{\Gamma}^i)$ are the main variables, and $\mathbf{A}^1$, $\mathbf{A}^2$, $\mathbf{A}^3$ and $\mathbf{B}$ are matrix-valued functions of $u$. Decomposing $Z_{ij} = \hat{Z}_{(ij)} + Z_{[ij]} + \gamma_{ij}Z/3$ into its trace-free symmetric part $\hat{Z}_{(ij)}$, its anti-symmetric part $Z_{[ij]}$, and its trace $Z = \gamma^{ij}Z_{ij}$ with respect to the physical three-metric $\gamma_{ij}$, and representing $C$ in terms of the variables $C = (C^i_\Gamma, S_1 := 2mH + Z, S_2 := H + 2\sigma Z, M_j, \hat{Z}_{(ij)}, Z_{[ij]})$, the principal symbol $\mathbf{A}(\mathbf{n}) = \mathbf{A}(u)^i n_i$ is given by

$$\begin{aligned}\mathbf{A}(\mathbf{n})C \;=\; \Big(&0, 0, n^j M_j\,, \frac{1}{3}n_j S_2 + \frac{1}{2}n^i\hat{Z}_{(ij)} + \frac{1}{2}n^i Z_{[ij]}\,,\\ &2(n_{(i}M_{j)})^{TF}, 2n_{[i}M_{j]}\Big),\end{aligned} \tag{2}$$

where $n^i \equiv \gamma^{ij}n_j$ and $n_i$ is normalized such that $n_i n^i = 1$. This system is symmetric hyperbolic, and its characteristic speeds (with respect to normal observers) are 0 and $\pm 1$. A symmetrizer is given by the quadratic form

$$\begin{aligned}C^T\mathbf{H}C \;=\; &\tilde{\gamma}_{ij}C^i_\Gamma C^j_\Gamma + S_1^2 + \frac{1}{3}S_2^2 + \gamma^{ij}M_i M_j\\ &+ \frac{1}{4}\gamma^{ik}\gamma^{jl}\hat{Z}_{(ij)}\hat{Z}_{(kl)} + \frac{1}{4}\gamma^{ik}\gamma^{jl}Z_{[ij]}Z_{[kl]}\,.\end{aligned}$$

The symmetrizer, along with the fact that there are no superluminal characteristic speeds, allow us to obtain an

[1] However, constraint violations can still be introduced by improper outer boundary conditions.

energy estimate for the constraint variables $C$ and to show that no constraint violations from the interior of a black hole can propagate to the outside. The explicit estimate will be presented elsewhere along with more details of the results presented in this paper.

## III. SINGLE BLACK HOLE EVOLUTIONS AND THE END STATE

In this section we present insights obtained by applying the turducken technique to a single spherically symmetric black hole. For these studies we use both the three–dimensional (3D) code described in section IV, as well as the one–dimensional (1D) BSSN code discussed in [23]. Both codes use a formulation of the BSSN equations that is strongly hyperbolic everywhere except in regions of the computational domain that are likely sets of measure zero, and have causal constraint propagation.

For a single black hole we use turduckened Kerr–Schild (KS) initial data. Without turduckening, a KS slice hits the singularity. We first define the spacetime metric $g_{\mu\nu} = \eta_{\mu\nu} + 2H\ell_\mu\ell_\nu$ in terms of Cartesian coordinates $x$, $y$, $z$, where $\eta_{\mu\nu}$ is the Minkowski metric, $H = M/\bar{r}$ and $\ell_\mu = (1, x, y, z)/\bar{r}$. Here, $\bar{r}$ is defined in terms of coordinate radius $r = (x^2 + y^2 + z^2)^{1/2}$ by $\bar{r} = (r^p + \epsilon^p)^{1/p}$. The contravariant metric $g^{\mu\nu}$ is obtained from $g_{\mu\nu}$ by raising indices with $\eta^{\mu\nu}$. In Cartesian coordinates the initial metric is defined by the spatial components of $g_{\mu\nu}$ and the initial extrinsic curvature is defined by the usual expression $K_{ij} = (-\dot{g}_{ij} + \beta^k\partial_k g_{ij} + 2g_{k(i}\partial_{j)}\beta^k)/2\alpha$, where $\alpha = 1/\sqrt{-g^{tt}}$ and $\beta^i = -g^{it}/g^{tt}$. The initial data for the 1D code is obtained by transforming the Cartesian data to spherical coordinates.

For $r \gg \epsilon$ we find $\bar{r} \approx r$ and the initial data coincides with a KS slice of a non–rotating black hole. For $r$ close to the origin, the data are smooth and regular as long as $\epsilon \neq 0$. This form of turduckening is not ideal since it leads to constraint violations that extend beyond the horizon $r = 2\,M$. Typical values used in our simulations are $\epsilon = 0.1M$ and $p = 4$. These values lead to initial violations of the Hamiltonian constraint of $\sim 10^4/M^2$ at $r = 0$ and $\sim 10^{-5}/M^2$ at $r = 2\,M$.

Experiments in 1D show that after an evolution time of $50\,M$, the Hamiltonian constraint violation throughout the computational domain drops to a level $\sim 10^{-5}/M^2$. Similar results hold for the other constraints. By $t = 50\,M$ the data have become nearly stationary; the final state in the $t \to \infty$ limit coincides with a portion of the stationary $1+\log$ slice of Schwarzschild. This is the same end state obtained with puncture evolution [8, 10]. The key ingredient responsible for these remarkable behaviors is the Gamma–driver shift condition. With this condition the shift grows large in the interior region to counteract the grid stretching that would otherwise occur as the lapse collapses. As a result the time flow vector field tips outside the physical light cone (toward increasing $r$) and the grid points near $r = 0$ are quickly driven out of causal contact with the constraint violating portion of the initial data. With the constraints (nearly) satisfied everywhere in the computational domain, the numerical data represents a slice of Schwarzschild that extends from region I of the Kruskal diagram, crosses the black hole horizon, and terminates at a resolution–dependent location inside the black hole. The $1+\log$ slicing condition then guides the slice to a stationary state.

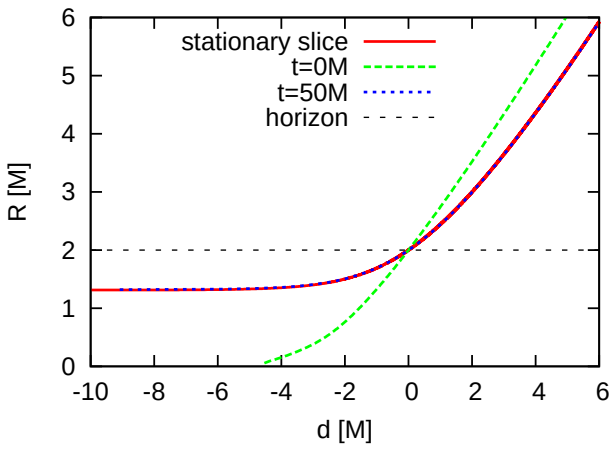


Figure 1: Areal radius $R$ versus proper distance $d$ from the horizon. The initially turduckened KS become indistinguishable from the portion $d \gtrsim -9$ of a stationary $1+\log$ slice after $t \approx 50\,M$. The region $R < 2\,M$ is the black hole interior.

Fig. 1 shows the areal radius $R$ versus proper distance $d$ (in the radial direction) for a single non–spinning black hole, obtained from the 1D code with resolution $M/200$. The data evolve to the stationary $1+\log$ slice in spite of the fact that the initial data violate the constraints.

Alternatively, the initial KS data can be changed only inside a sphere of radius $r_0 < 2M$. In 1D simulations such initial data can lead to the formation of gauge shocks, like those discussed in [9]. The shocks typically form just outside the black hole, independent of the parameter $r_0$; this suggests that the formation of shocks is a consequence of the gauge conditions, and not the black hole turduckening. We have not seen this behavior in 3D, perhaps due to lack of resolution.

## IV. BINARY BLACK HOLE EVOLUTIONS USING COOK-PFEIFFER DATA

We evolve quasi-equilibrium binary black hole initial data using the form of the equations described above, implemented in `CCATIE`, a three-dimensional adaptive mesh refinement code which uses the Cactus framework [24] and the Carpet mesh refinement driver [25, 26]. This evolution code is fourth order accurate. It uses centered finite differencing operators, except for the advection terms which are upwinded. We use fifth order spatial and second order temporal polynomial interpolation at mesh refinement boundaries, and buffer zones as de-

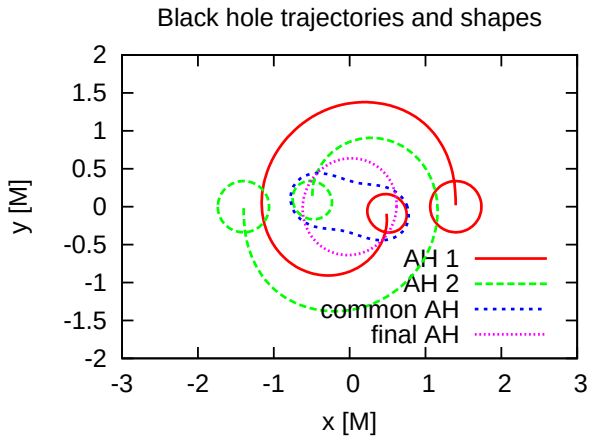


Figure 2: Apparent horizons in a binary black hole evolution of Cook-Pfeiffer data. This figure shows the tracks of the centroids of the apparent horizons, as well as their shapes at $t = 0\,M$, at merger ($t \approx 37\,M$), and at late times ($t \geq 200\,M$).

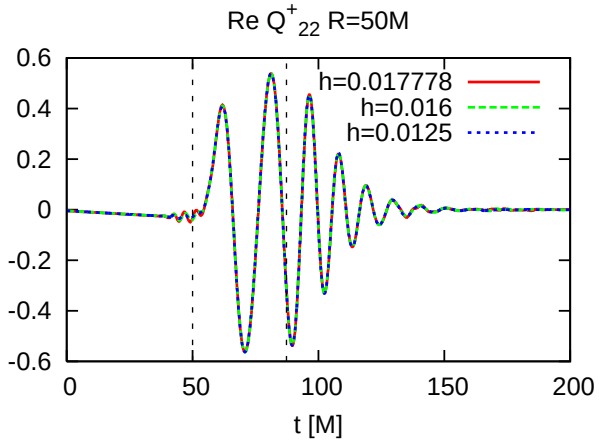


Figure 3: Real part of the waveform $Q^+_{22}$, extracted at $R = 50\,M$. The vertical lines indicate approximately when the initial burst of spurious radiation first reaches the detector and when the common horizon is "seen" by the detector. The "junk" radiation near $t = 50\,M$ is a well-known feature from puncture evolutions.

scribed in [25] to ensure stability. We therefore expect our code to be third order accurate in the limit of infinite resolution, and expect it to show approximate fourth order convergence away from the outer boundary and for the resolutions used here. We use a fourth order Runge-Kutta time integrator with a CFL factor of 0.4. We use Sommerfeld outer boundary conditions for the individual components of the evolved variables, which are not constraint preserving; we therefore place the outer boundaries at a large distance from the source.

The initial data were provided by Harald Pfeiffer [27] and are described in [28, 29]. In particular we use the data set `sep_07.00_59a.tgz` in which the binary black hole system is expected to orbit approximately once before merging. These data have an ADM mass $M_{\rm ADM} \approx 2.44449 \approx 0.977795\,M$, where we use a scale factor $M = 2.5$. The black holes are centered about $x = \pm 1.4\,M$, and the apparent horizons have a coordinate radius $r_{\rm AH} \approx 0.35\,M$.

Our simulations use reflection symmetry about $z = 0$ and $\pi$-rotation symmetry about the $z$ axis. We choose a simulation domain with outer boundaries at $204.8\,M$, and use altogether 9 successively smaller levels of mesh refinement, where the finest level has an extent of $0.8\,M$, centered about each black hole. Our resolution is $h = 3.2\,M$ on the coarsest grid, $h = 0.8\,M$ near the gravitational wave detector, and $h = 0.0125\,M$ on the finest grid. We include results from two coarser runs with coarse grid resolutions $h \approx 4.5\,M$ and $h \approx 4.1\,M$, respectively.

The initial data are provided in terms of spectral expansion coefficients for the ADM variables on multiple domains and need to be interpolated to our grid points. The initial data setup excises the apparent horizons but extrapolates a distance of up to $0.25\,r_{\rm AH} = 0.0875\,M$ into the horizon. The remainder of the interior of the apparent horizons needs to be turduckened.

We have experimented with various methods for turduckening the black hole interior, and find that the details do not matter much in practice, as long as the spacetime remains unchanged within the finite differencing stencil radius of the horizon. Since there are preciously few grid points between the excised region and the horizon, we chose a method which leaves all given spacetime data unchanged and fills in the excised points in a smooth manner. (One alternative would be a blending method which fills the excised region with arbitrary data, and then modifies some of the non-excised grid points to create a smooth match.)

In particular, we solve the elliptic equation $(\partial^6/\partial x^6 + \partial^6/\partial y^6 + \partial^6/\partial z^6)A = 0$ to fill the excised points of a quantity $A$, using standard centered derivatives everywhere and using the given non-excised data as boundary conditions where necessary. This is equivalent to providing boundary conditions for $A$ and its normal derivatives $\partial A/\partial \mathbf{n}$, and $\partial^2 A/\partial \mathbf{n}^2$. The result is therefore $C^2$ everywhere within the horizon. We solve this equation with a standard conjugate gradient method.

We follow the evolution of these data through merger and ringdown for about $200\,M$. Fig. 2 shows the locations, shapes, and tracks of the individual and the common apparent horizons. A common horizon appears at about $t = 37\,M$. The common horizon initially has a strong $Y_{22}$ deformation which is radiated away. This is clearly shown in the real part of the $\ell = m = 2$ mode of the Zerilli function $Q^+$, extracted on a coordinate sphere at $R = 50\,M$ and shown in Fig. 3. Fig. 4 shows the results of a convergence test, although the resolutions are too close together to give reliable results. Both the horizon dynamics and waveforms are very similar to those from puncture initial data. We will present a study of this and other systems with larger initial separations in more detail elsewhere.

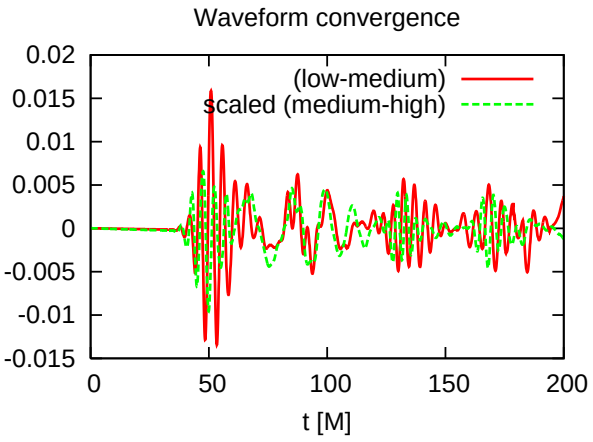


Figure 4: Difference between waveforms, scaled for 4th order convergence. The waveform phases have been shifted in time so that all resolutions have the same phase at the beginning of the merger radiation burst at $t \approx 60\,M$. The initial high-frequency oscillations in the error are caused by the small amount of "junk" radiation near $t = 50\,M$, and similar oscillations near $t = 140\,M$ are probably caused by its reflection at the coarsest refinement level. The noise near $t = 170\,M$ appears at a time when the waveform has already rung down.

## V. FINAL REMARKS

A key property needed in a "free black hole evolution" approach is that the constraints propagate causally. This cannot be taken for granted, and must be proved (or tested) for any particular formulation of the Einstein equations used. Note that even apparently small variations in the evolution system can change the constraint propagation from causal to acausal.

Causal propagation of the constraints alone is not sufficient. In modifying the initial data by smoothing away the singularity, we are not guaranteeing that the evolution will proceed to a smooth, regular end-state. That this end-state is numerically well-behaved is the other key ingredient in any evolution that relies on modifying the interior of the horizon in some way. As the numerical evidence presented here shows, evolutions in spherical symmetry do tend to a recognizable end-state for the given set of gauge conditions and form of the equations. It seems likely that a similar picture will hold away from spherical symmetry.

Our work suggests that the turducken technique will hold irrespective of how and when the data inside the horizon are modified, thus allowing the method to be applied without modification to the final stages of evolutions performed with possibly different codes and/or methods, or to horizons formed e.g. in stellar collapse scenarios.

Most of the results of this paper were originally presented [30] by one of us (ES) at the Tenth Eastern Gravity Meeting. Since then, and while completing this paper, independent results complementary to those presented here have been presented in Ref. [31].

### Acknowledgments

We thank H. Pfeiffer for making the initial data available to us, and for his help in implementing a reader for these data. OS thanks D. Nuñez for help in deriving the characteristic speeds and fields of the constraint propagation system. MT thanks S. Teukolsky for hospitality at Cornell University, where part of this work was done. We employ J. Thornburg's apparent horizon finder [32]. This research was supported in part by NSF grant PHY 0505761 and NCSA grant MCA02N014 to Louisiana State University, and by NSF grant PHY 0600402 to North Carolina State University. We use the supercomputing resources Peyote at the AEI, Eric at LONI, Supermike at LSU, and Abe and Tungsten at the NCSA. We also employ the resources of the CCT at LSU, which is supported by funding from the Louisiana legislature's Information Technology Initiative.

[1] J. Thornburg, Class. Quantum Grav. **4**, 1119 (1987).
[2] W. G. Unruh (1984), personal communication to J. Thornburg.
[3] M. Campanelli, et al., Phys. Rev. Lett. **96**, 111101 (2006).
[4] J. G. Baker, et al., Phys. Rev. Lett. **96**, 111102 (2006).
[5] F. Pretorius and D. Khurana, Class. Quantum Grav. **24**, S83 (2007).
[6] H. P. Pfeiffer, et al., Class. Quantum Grav. **24**, S59 (2007).
[7] M. Hannam, et al. (2007), arXiv:0706.1305 [gr-qc].
[8] J. D. Brown (2007), arXiv:0705.1359 [gr-qc].
[9] D. Garfinkle, C. Gundlach, and D. Hilditch, arXiv:0707.0726 [gr-qc].
[10] M. Hannam, et al. (2006), gr-qc/0606099.
[11] A. Arbona, et al., Phys. Rev. D **57**, 2397 (1998).
[12] C. Bona, et al. (2004), gr-qc/0410079.
[13] A. Arbona, et al., Phys. Rev. D **60**, 104014 (1999).
[14] C. W. Misner (2001), URL `https://drum.umd.edu/dspace/handle/1903/4361`.
[15] `http://en.wikipedia.org/wiki/Turducken`.
[16] H. Beyer and O. Sarbach, Phys. Rev. D **70**, 104004 (2004).
[17] M. Alcubierre, et al., Phys. Rev. D **67**, 084023 (2003).
[18] J. R. van Meter, et al., Phys. Rev. D **73**, 124011 (2006).
[19] H. O. Kreiss and O. E. Ortiz, Lect. Notes Phys. **604**, 359 (2002).
[20] G. Nagy, O. E. Ortiz, and O. A. Reula, Phys. Rev. D **70**, 044012 (2004).
[21] G. Calabrese, et al., Comm. Math. Phys. **240**, 377 (2003).

[22] O. Sarbach and M. Tiglio, Phys. Rev. D **66**, 064023 (2002).
[23] J. D. Brown (2007), arXiv:0705.3845 [gr-qc].
[24] URL `http://www.cactuscode.org/`.
[25] E. Schnetter, S. H. Hawley, and I. Hawke, Class. Quantum Grav. **21**, 1465 (2004).
[26] URL `http://www.carpetcode.org/`.
[27] URL `http://www.black-holes.org/researchers3.html`.
[28] G. B. Cook and H. P. Pfeiffer, Phys. Rev. D **70** (2004).
[29] H. P. Pfeiffer, et al., Comput. Phys. Commun. **152**, 253 (2003).
[30] URL `http://baba.astro.cornell.edu/~ecgm10/`.
[31] Z. B. Etienne, et al., arXiv:0707.2083 [gr-qc].
[32] J. Thornburg, Class. Quantum Grav. **21**, 743 (2004).